Journal of Chromatography, 595 (1992) 237–246
Elsevier Science Publishers B.V., Amsterdam

CHROM. 23 915

Activity coefficients in binary liquid mixtures measured by reversed-flow gas chromatography

A. Koliadima, G. Karaiskakis* and N. A. Katsanos

Physical Chemistry Laboratory, University of Patras, 26110 Patras (Greece)

M. Roth

Institute of Analytical Chemistry, Czechoslovak Academy of Sciences, 61142 Brno (Czechoslovakia)

(First received July 8th, 1991; revised manuscript received November 20th, 1991)

ABSTRACT

Three methods of reversed-flow gas chromatography are presented for the determination of activity coefficients in binary liquid mixtures. The systems used were *n*-hexane–*n*-hexadecane and benzene–*n*-octane. The average activity coefficients obtained for *n*-hexane in the first system were close to those given in the literature, when the *n*-hexane mole fraction was close to unity, whereas the values found for benzene in the second system were close to those calculated theoretically, using the Margules equation, when the benzene mole fraction approached zero or unity. On the other hand, the activity coefficients of *n*-octane in the same system were close to the theoretical values only when the *n*-octane mole fraction was close to unity. All these deviations are discussed and possible causes, such as liquid diffusion, fugacity correction and thermal non-equilibrium considered.

INTRODUCTION

The reversed-flow gas chromatography method (RF-GC) has been reviewed several times [1–4], and some more recent papers have been cited [5]. Some of them refer to the determination of activity coefficients in solution [6–8], and are based on a theoretical analysis published in 1984 [9].

It is well known that flow reversals of the carrier gas at various times t_0, by means of a four- or six-port valve (*cf.*, Fig. 1), execute repeated sampling at the junction $x = l'$ of concentration $c(l', t_0)$ of the substances present at this point at t_0. This sampling results in extra chromatographic peaks (sample peaks), such as those shown in Fig. 2. The magnitude of $c(l', t_0)$ in each sampling act is related to the height h of the respective sample peak by the equation [4]

$$h = [2c(l', t_0)]^m \quad (1)$$

where m is the response factor of the detector. For a flame ionization detector, $m = 1$.

The function $c = c(l', t_0)$ has been derived in the past for many special cases pertaining to various physico-chemical parameters and different experimental conditions. One particular case is closely related to the present problem and is given by eqns. 14 and 18 in ref. 9. These equations are a short and a long time approximation, respectively, and apply when a vessel of height L_2 (*cf.*, Fig. 1) contains a pure liquid. The same analysis was employed [6–8] when two- or more component mixtures were placed in a vessel of height y. It is the purpose of this paper to elaborate and extend the theoretical analysis, so that a single equation embraces short and long time in the same experiment.

It is shown in the Appendix that the general solution, based on eqn. 1, takes the form:

$$h = h_\infty - A_1 \exp[-(\alpha + \omega)t_0] + A_2 \exp(-9\alpha t_0) \quad (2)$$

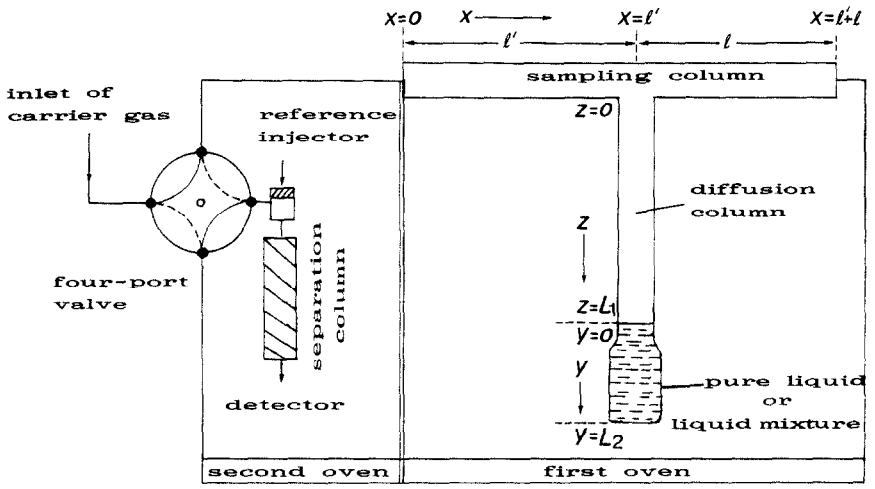

Fig. 1. Experimental set-up for measuring activity coefficients in binary liquid mixtures by RF-GC.

where

$$h_\infty = \frac{2k\alpha}{\alpha + \omega} = \frac{2k_c c_0 a_L}{a_G u} \cdot \frac{\alpha}{\alpha + \omega} \tag{3}$$

$$A_1 = 2k\left(\frac{4}{\pi} - 1 + \frac{\alpha}{\alpha + \omega} + \frac{4}{3\pi} \cdot \frac{\omega}{8\alpha - \omega}\right) \tag{4}$$

$$A_2 = 2k \cdot \frac{4}{3\pi} \cdot \frac{8\alpha}{8\alpha - \omega} \tag{5}$$

$$k = k_c c_0 a_L / a_G u \tag{6}$$

$$\alpha = \pi^2 D / 4L_1^2 \tag{7}$$

$$\omega = 2k_c a_L / a_G L_1 \tag{8}$$

where k_c is the mass transfer coefficient for the liquid evaporation, c_0 is the concentration of the vapour which would be in equilibrium with the bulk liquid phase, a_L is the free surface area of the liquid, a_G is the cross-sectional area of the column with height z (*cf.*, Fig. 1), u is the linear velocity of the carrier gas in the sampling column and D is the diffusion coefficient of the vapour into the gases contained in column z, *viz.*, the carrier gas and other vapours.

EXPERIMENTAL

The solutes used were *n*-hexane (pure) and *n*-hexadecane (GC grade, purity >99%) from Merck, *n*-octane (purum) from Fluka and benzene (pure) from Carlo Erba. The nitrogen carrier gas (Linde) had a purity of ≥99.99%. The chromatographic material for the separation of the components of the mixtures, which was filled into a 64.5-cm separation column, was 11% Apiezon M on Chromosorb P AW DMCS (60–80 mesh).

The apparatus used and the experimental procedure followed have been described in detail elsewhere [8,9]. A conventional gas chromatograph (Pye Unicam Series 104) contained in its oven the sampling column, consisting of two sections of lengths $l' + l = 100 + 100$ cm and the diffusion column with length $L_1 = 114.8$ cm. At the lower end of diffusion column a glass tube ($L_2 = 2.5$ cm) containing the pure liquid or the liquid mixture was connected. One end of the sampling column was connected to the carrier gas supply and the other end to the separation column, which was placed in a second gas chromatographic oven. The end of this column was connected to a flame ionization detector as shown schematically in Fig. 1.

At a given time after placing the pure liquid or the liquid mixture in position, an asymmetric concentration–time curve for the detected vapours was recorded, rising continuously and approaching a limiting plateau. This concentration *vs.* time curve consists of one substance (in the *n*-hexane–*n*-hexadecane system where the vapour pressure of *n*-hexadecane is negligible at the working temperature)

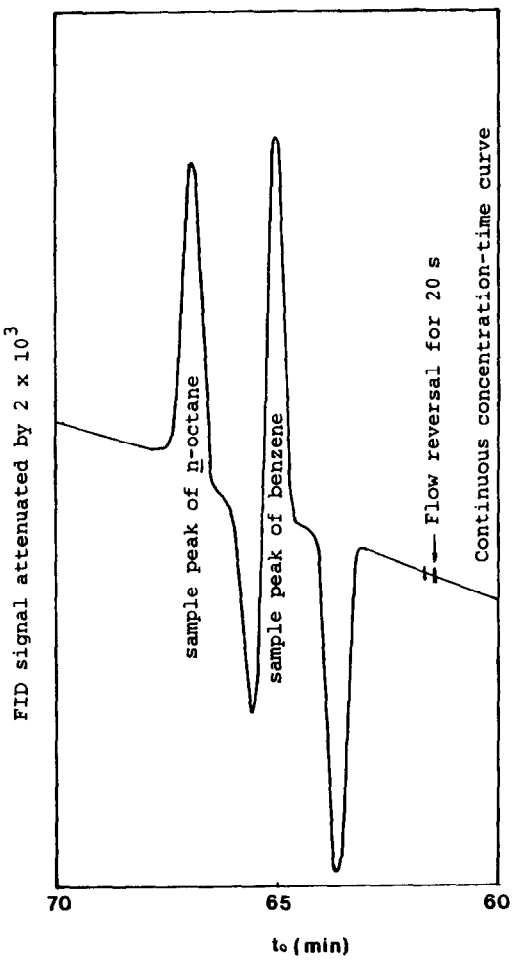

Fig. 2. A reversed-flow chromatogram, showing two sample peaks for the diffusion of benzene and *n*-octane vapours into nitrogen carrier gas at 348.2 K and 1 atm.

or of two substances (in the benzene–*n*-octane system). During the rise period, and also when the plateau was reached, flow reversals for 20 s were effected by means of the four-port valve. When the gas flow was restored to its original direction, one or two sample peaks were recorded (*cf.*, Fig. 2) corresponding to various times t_0 from the beginning.

The carrier gas flow-rate was kept constant in all runs at 0.4 cm^3 s^{-1} (at ambient temperature). The working temperature was 348.2 K for the evaporation of the mixtures (first oven) and 393.2 K for the separation column (second oven). The pressure drop along the whole system of columns was negligible.

RESULTS AND DISCUSSION

There are three obvious procedures for analysing the experimental data by means of eqn. 2, as follows.

First procedure

The experimental value of h_∞, established after a sufficiently long time, is used and a plot of ln $(h_\infty - h)$ *vs.* t_0 is constructed according to the following form of eqn. 2:

$$h_\infty - h = A_1 \exp[-(\alpha + \omega)t_0] - A_2 \exp(-9\alpha t_0) \quad (9)$$

An example is given in Fig. 3. As predicted by the equation, this plot becomes linear after a certain time, because the second exponential has decayed to a negligible value, giving

$$\ln (h_\infty - h) = \ln A_1 - (\alpha + \omega)t_0 \quad (10)$$

Having found $\alpha + \omega$ from the slope and A_1 from the intercept of this linear part of the plot, one replots the initial data as

$$\ln \{A_1 \exp[-(\alpha + \omega)t_0] - (h_\infty - h)\} = \ln A_2 - 9\alpha t_0 \quad (11)$$

and finds α from the slope and A_2 from the intercept of the new plot.

Second procedure

Pairs of values h_2 and h_1 are used, measured at equidistant times t_2 and t_1, respectively, *i.e.*, with $\Delta t = t_2 - t_1 =$ constant. Then eqn. 2 gives, on writing it twice, subtracting and rearranging,

$$h_2 - h_1 = A'_1 \exp[-(\alpha + \omega)t_1] - A'_2 \exp(-9\alpha t_1) \quad (12)$$

where

$$A'_1 = A_1\{1 - \exp[-(\alpha + \omega)\Delta t]\} \quad (13)$$

and

$$A'_2 = A_2[1 - \exp(-9\alpha \Delta t)] \quad (14)$$

A plot of ln $(h_2 - h_1)$ *vs.* t_1 is constructed (*cf.*, Fig. 4), which after some time is approximated by

$$\ln (h_2 - h_1) = \ln A'_1 - (\alpha + \omega)t_1 \quad (15)$$

Having found $\alpha + \omega$ from the slope and A'_1 from the intercept of this linear part, we replot the initial data as

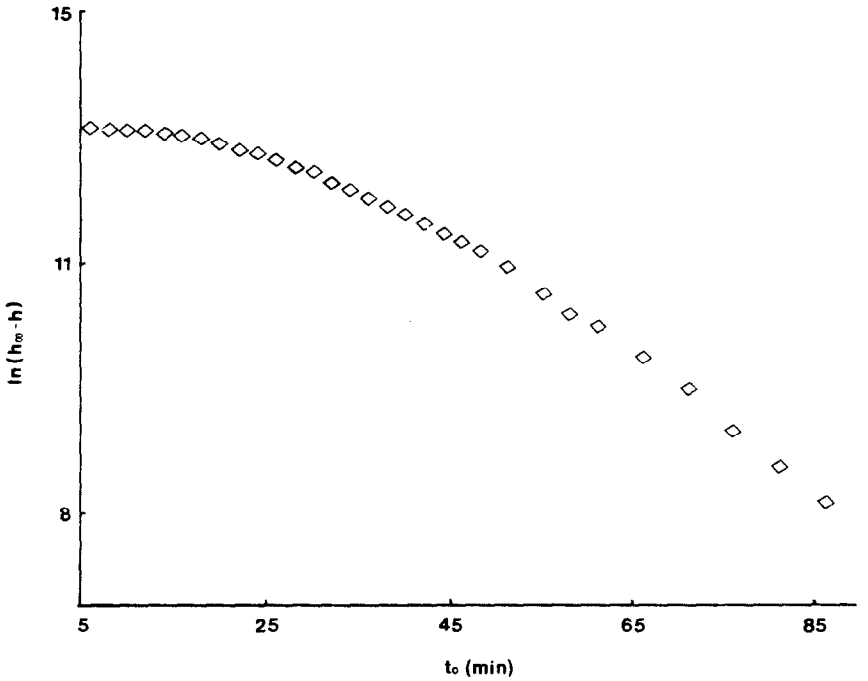

Fig. 3. Example of plotting eqn. 9 for the diffusion of *n*-hexane vapour into nitrogen carrier gas ($\dot{V} = 0.4\,cm^3\,s^{-1}$) at 348.2 K and 1 atm.

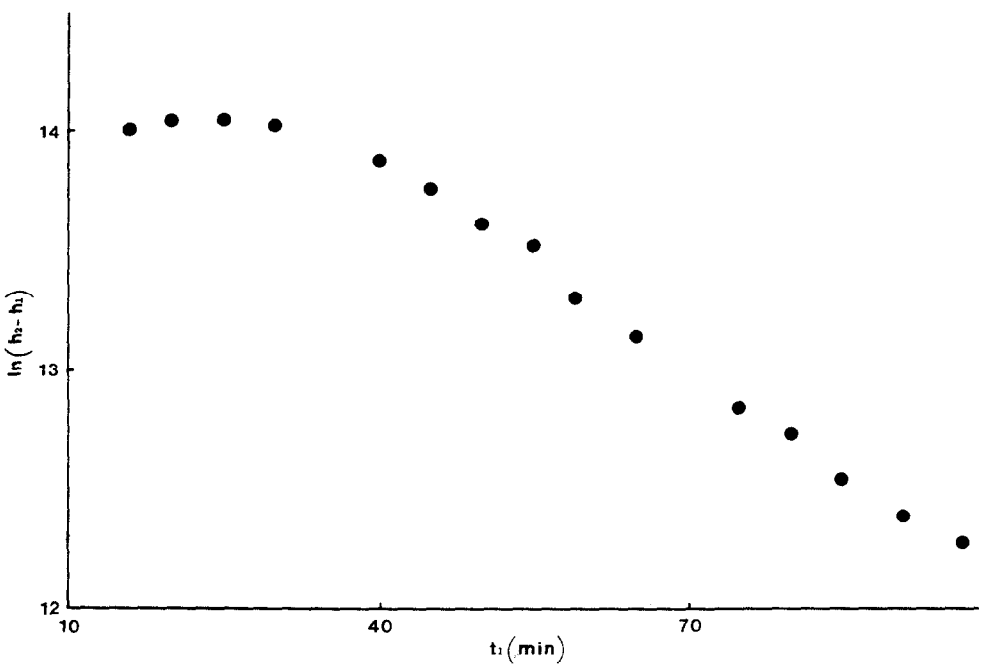

Fig. 4. Example of plotting eqn. 12 for the diffusion of benzene vapour into nitrogen carrier gas ($\dot{V} = 0.4\,cm^3\,s^{-1}$) at 348.2 K and 1 atm.

$$\ln\{A'_1 \exp[-(\alpha + \omega)t_1] - (h_2 - h_1)\} = \ln A'_2 - 9\alpha t_1 \quad (16)$$

and we find α and A'_2 from the slope and the intercept, respectively, of the new plot.

The value of h_∞ can now be calculated from eqn. 2 by substituting in it any pair of h, t_0 values, as A_1, $\alpha + \omega$, A_2 and 9α are all known from the above plots, using also eqns. 13 and 14 and the known value of Δt.

Third procedure

Differentiating eqn. 2 with respect to time, we obtain

$$\frac{dh}{dt_0} = A_1(\alpha + \omega)\exp[-(\alpha + \omega)t_0] - 9\alpha A_2 \exp(-9\alpha t_0) \quad (17)$$

The plot of the experimental data this time should be of ln (dh/dt_0) *vs.* t_0 (*cf.*, Fig. 5), dh/dt_0 being calculated approximately from $\Delta h/\Delta t_0 = (h_2 - h_1)/(t_2 - t_1)$, with t_2 and t_1 as close to each other as possible, and $t_0 = (t_1 + t_2)/2$. Again, this plot, according to eqn. 17, should become after some time

$$\ln(dh/dt_0) = \ln[A_1(\alpha + \omega)] - (\alpha + \omega)t_0 \quad (18)$$

and before this

$$\ln\{A_1(\alpha + \omega)\exp[-(\alpha + \omega)t_0] - dh/dt_0\} = \ln(9\alpha A_2) - 9\alpha t_0 \quad (19)$$

Therefore, as in the previous two procedures, $\alpha + \omega$, A_1, α and A_2 can easily be calculated from the slopes and the intercepts of the two plots described above by eqns. 18 and 19.

It should be noted that when Δt in the second procedure is small, eqn. 12 leads to eqn. 17 with $dh/dt_0 = (h_2 - h_1)/\Delta t$. This is done by expanding the exponentials of eqns. 13 and 14 in MacLaurin series and retaining only the first two terms.

The activities and activity coefficients can be calculated from (a) the experimental h_∞ given by eqn. 3; (b) the A_1 or A_2 values found in the first procedure and given by eqns. 4 and 5, respectively; (c) the A'_1 or A'_2 values found in the second

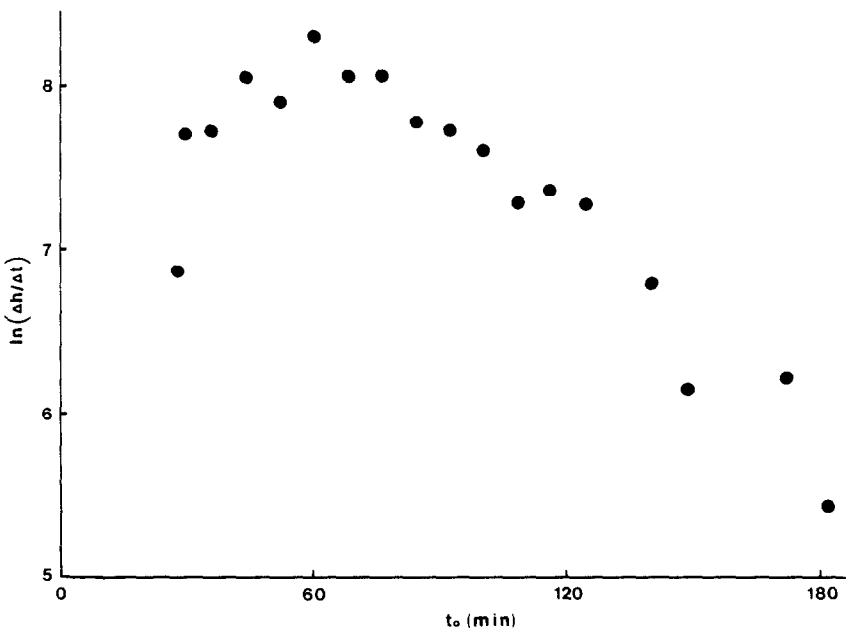

Fig. 5. Example of plotting eqn. 17 for the diffusion of benzene vapour from the benzene–*n*-octane system ($x_1 = 0.5$) into nitrogen carrier gas ($\dot{V} = 0.4$ cm^3 s^{-1}) at 348.2 K and 1 atm.

procedure and given by eqns. 13 and 14, respectively; (d) the A_1 ($\alpha + \omega$) or $9\alpha A_2$ of eqn. 17 in the third procedure. All these parameters contain $k = k_c c_0 a_L / a_G u$ as given by eqn. 6, with k_c being determined from the value of ω (*cf.*, eqn. 8).

Fig. 6 shows the variation of the average activities, as determined by methods (a), (b), (c) and (d) above, of *n*-hexane in the *n*-hexane (1)–*n*-hexadecane (2) system, and of the corresponding literature activities [10] with the *n*-hexane mole fraction. It is seen that the experimental activities, a_1, approach the corresponding literature values only when the *n*-hexane mole fraction approaches unity ($x_1 = 0.93$). This may be due to the fact that either the binary liquid mixtures are not completely homogeneous at the low range of composition or their low composition does not remain constant during the evaporation process. Another possible explanation of this finding may be the diffusion of *n*-hexane into liquid *n*-hexadecane, which was considered negligible in the theoretical treatment.

Let us now examine whether the stirring of the liquid mixture, and hence the liquid diffusion, influences the activities or activity coefficients determined. The experimental activity coefficients, based on the first procedure, for *n*-hexane ($\gamma_1 = 0.842$ with stirring and $\gamma_1 = 0.852$ without stirring) support the hypothesis in the Appendix that the liquid diffusion is negligible. The significance or not of the liquid diffusion with respect to the activity or activity coefficient determination was also examined by changing the volume of the liquid mixture, V. The results, obtained again in the first way ($\gamma_1 = 0.842$ with $V = 1.96$ cm^3 and $\gamma_1 = 0.784$ with $V = 2.72$ cm^3) are not very different, showing that liquid diffusion does not significantly influence the evaporation process of *n*-hexane from the *n*-hexane–*n*-hexadecane system. Comparison of all the *n*-hexane activities, determined by the above four methods at the composition $x_1 = 0.93$, in which the average experimental activity approaches the literature value, with that actually found in the literature [10] shows that method (c) of activity determination is more accurate. On the other hand, comparison of the average diffusion coefficients of the *n*-hexane vapour into the carrier gas nitrogen, calculated from eqn. 7 for the three methods used ($D = 0.386$ cm^2 s^{-1} with the first, $D = 0.488$ cm^2 s^{-1} with the second and $D = 0.834$ cm^2 s^{-1} with the third procedure), with that ($D = 0.388$ cm^2 s^{-1}) obtained by the Füller–Schettler–Giddings (FSG) method [11], shows that the more accurate method, at least

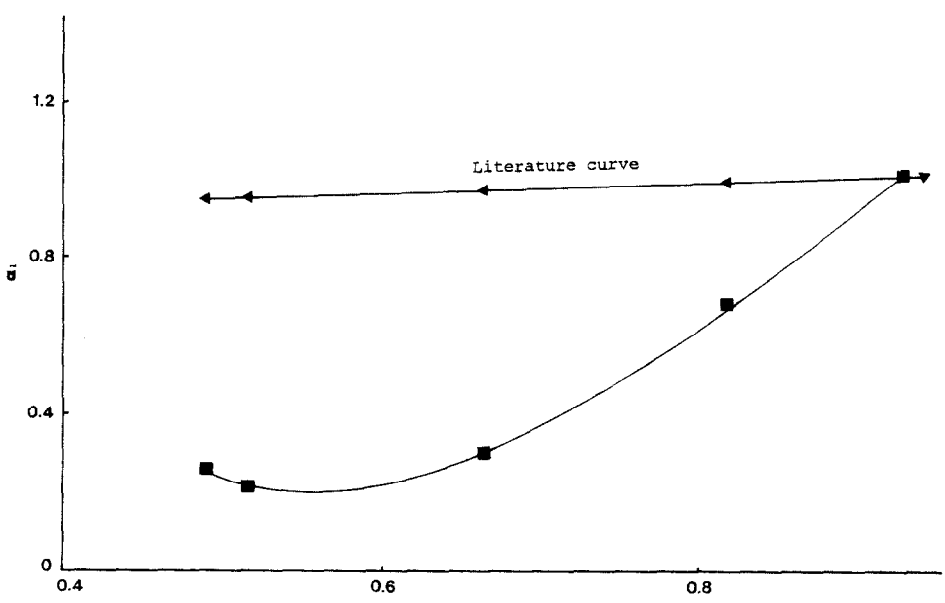

Fig. 6. Variation of the average experimental activities, a_1, of *n*-hexane in the *n*-hexane (1)–hexadecane (2) system, and of the literature activities, with the *n*-hexane mole fraction ($T = 348.2$ K, $P = 1$ atm, $\dot{V} = 0.4$ cm^3 s^{-1}).

for the diffusion coefficient determination, is that based on the first procedure above. This conclusion is supported by the fact that the values of the mass transfer coefficients, $k_{c'}$, determined by the first procedure are closer to those obtained in a previous study [9].

Fig. 7 shows the variation of the benzene average values for activity a_1 in the benzene (1)–*n*-octane(2) system, determined by the four methods mentioned, with the benzene mole fraction, and also the variation of the corresponding theoretical activities with the composition of the mixture. The latter were calculated by the three-suffix Margules equation, resulting from the experimental vapour–liquid equilibrium data [12] for the benzene–*n*-octane system at the working temperature (T = 348.2 K). This equation has the form

$$\ln \gamma_1 = [A_{12} + 2(A_{21} - A_{12})x_1]x_2^2 \quad (20)$$

$$\ln \gamma_2 = [A_{12} + 2(A_{12} - A_{21})x'_2]x_1^2 \quad (21)$$

The constants of eqns. 20 and 21, which at T = 348.2 K have the values A_{12} = 0.3516 and A_{21} = 0.4132, were taken from ref. 13.

It can be seen from Fig. 7 that the average experimental activities of benzene approach the theoretical values, calculated from eqn. 20, as the benzene mole fraction approaches unity or zero. The case when $x_1 \rightarrow 1$ is similar to that found for *n*-hexane in the *n*-hexane–*n*-hexadecane system, and is probably due to the same reasons. The second case ($x_1 \rightarrow 0$), which means that the solute component is at infinite dilution, is the ideal condition for studying interactions in solutions by gas chromatography.

Comparison of the activities of benzene in the benzene–*n*-octane system obtained by the three ways

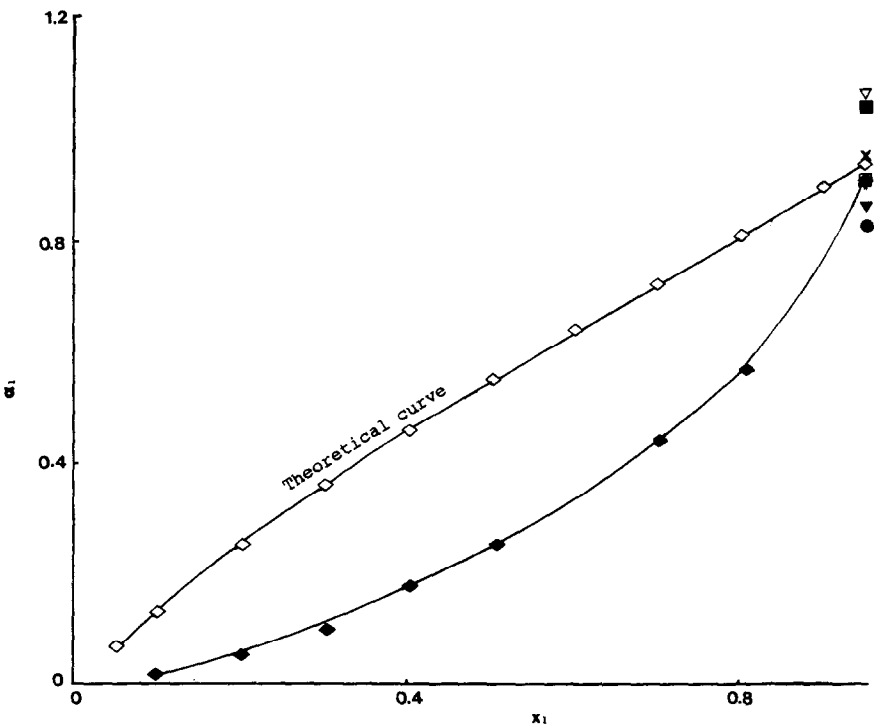

Fig. 7. Variation of average activities, a_1, as determined by the three methods of RF-GC presented, of benzene in the benzene–*n*-octane system, and of the theoretical activities, a_1, as determined from the Margules equation, with the benzene mole fraction (T = 348.2 K, P = 1 atm, $\dot{V}$ = 0.4 cm^3 s^{-1}). First method, × from h_∞, □ from A_1, # from A_2; second method, ■ from A_1, ▽ from A'_2; third method, ▼ from $A_1(\alpha + \omega)$, ● from $9\alpha A_2$; ◆, average values.

mentioned at the higher benzene mole fraction ($x_1 = 0.95$) with that calculated by eqn. 20, and of the average diffusion coefficients for benzene vapour into the carrier gas nitrogen ($D = 0.424$ cm^2 s^{-1} with the first, $D = 1.017$ cm^2 s^{-1} with the second and $D = 0.878$ cm^2 s^{-1} with the third procedure) with that obtained by the FSG method ($D = 0.464$ cm^2 s^{-1}) shows that the accuracy is again better for the method based on the first procedure.

The average experimental activities of *n*-octane, a_2, in the benzene–*n*-octane system, with the corresponding theoretical activities calculated from eqn. 21 at various compositions of the mixture are presented in Fig. 8. It can be seen that the experimental activities approach the theoretical values only when the *n*-octane mole fraction approaches unity. When $x_2 \rightarrow 0$ the experimental activities deviate strongly from the theoretical values, as at the working temperature ($T = 348.2$ K) and in this range of mixture composition the heights of the *n*-octane peaks are too low because of its low vapour pressure.

An effort to draw any conclusion from Fig. 8 regarding the accuracy of the three procedures used was unsuccessful, as the experimental data appear with a large random error.

The deviations pointed out earlier for the activities of *n*-hexane in the *n*-hexane–*n*-hexadecane system and of benzene or *n*-octane in the benzene–*n*-octane system can also be attributed to the effect of the thermal non-equilibrium, as the vessel with height L_2 (*cf.*, Fig. 1) is filled with the liquid mixture at the ambient temperature and needs some time to attain thermal equilibrium.

Finally, one can take into account the fugacity correction for the activities or activity coefficients determined. The fugacity correction for the activity coefficient of *n*-hexane in *n*-hexadecane was calculated using the second virial coefficients of *n*-hexane and the *n*-hexane–nitrogen second cross-virial coefficients obtained by fitting the respective literature data [14] with the Tsonopoulos correlation [15]. For the mixture *n*-hexane–*n*-hexadecane at 333.5 K and an *n*-hexane mole fraction of 0.818, the fugacity-corrected activity of *n*-hexane is 0.713, whereas the fugacity-uncorrected activity is 0.696. Hence the corrected value exceeds the uncorrected one by *ca.* 2.5%, which certainly cannot explain the difference between our results and the literature values, although the fugacity correction should increase as the mole fraction of *n*-hexane decreases. Obviously, more experimental work is necessary in order to investigate these anomalous deviations.

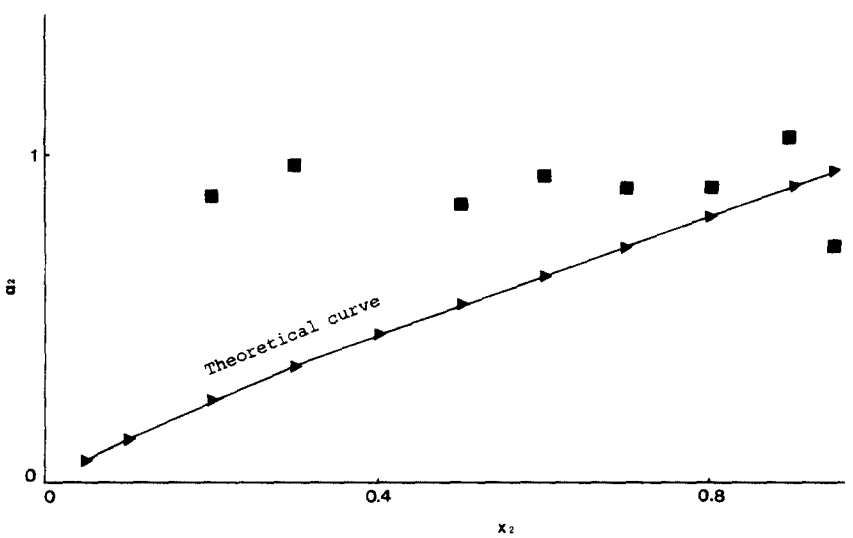

Fig. 8. Plot of the average experimental, a_2, and theoretical activities of *n*-octane in the benzene–*n*-octane system *vs.* the *n*-octane mole fraction ($T = 348.2$ K, $P = 1$ atm, $\dot{V} = 0.4$ cm^3 s^{-1}).

As a general conclusion, it may be said that the three methods of RF-GC presented here should give, under experimental conditions (the evaporation temperature of the solute to be close to its boiling point and the solute mole fraction to be close to zero or unity), activities or activity coefficients for binary liquid mixtures close to those obtained by other techniques or calculated theoretically. The first method appears to be the most accurate, yielding activities, diffusion coefficients and mass transfer coefficients closest to the theoretical values. However, this study shows that there can be differences in the reliability of the results depending on the approach used.

ACKNOWLEDGEMENT

The authors thank Mrs. Margaret Barkoula for assistance.

APPENDIX

The general solution in the form of eqn. 2 will be derived with the help of the coordinates of Fig. 1. The diffusion of a vapour leaving the liquid in vessel L_2 is described by the equation

$$\partial c_z/\partial t_0 = D\partial^2 c_z/\partial z^2 \tag{A1}$$

The initial condition is $c_z(z, 0) = 0$, and the boundary conditions at $z = 0$ are

$$c_z(0, t_0) = c(l', t_0) \quad \text{and} \quad D(\partial c_z/\partial z)_{z=0} = uc(l, t_0) \tag{A2}$$

The boundary condition at the other end, $z = L_1$, of the diffusion column is

$$Da_G(\partial c_z/\partial z)_{z=L_1} = k_c a_L[c_0 - c_z(L_1)] \tag{A3}$$

where $C_z(L_1)$ is the actual concentration at the liquid interface.

When the Laplace transform of eqn. A1 is taken with respect to t_0, a linear second-order differential equation results, and this is solved by using z Laplace transformation, giving

$$C_z = C_z(0)\cosh qz + \frac{C'_z(0)}{q}\sinh qz \tag{A4}$$

where

$$q^2 = p_0/D \tag{A5}$$

and $C_z(0)$ and $C'_z(0)$ are the t_0 Laplace transforms of $c_z(0)$ and $(\partial c_z/\partial z)_{z=0}$, respectively. Using the boundary conditions expressed by eqn. A2, eqn. A4 becomes

$$C_z = C(l', p_0)(\cosh qz + \frac{u}{Dq}\sinh qz) \tag{A6}$$

where $C(l', p_0)$ is the t_0 transformed function $c(l', t_0)$, which we try to express as an analytical function of time.

By means of eqn. A6, $C_z(L_1)$ and $(\partial C_z/\partial z)_{z=L_1}$ can be calculated and then substituted into eqn. A3 after the latter has been transformed with respect to t_0. The result is simplified by making the usual approximation to omit $\sinh qL_1$ compared with $(u/Dq)\cosh qL_1$ and $\cosh qL_1$ compared with $(u/Dq)\sinh qL_1$. These are valid for sufficiently high flow-rates. Subsequently we obtain

$$C(l', p_0) = k \cdot \frac{1}{p_0 \cosh qL_1} \cdot \frac{1}{1 + (k'_c/Dq)\tanh qL_1} \tag{A7}$$

where $k'_c = k_c a_L/a_G$ and k is given by eqn. 6.

Inverse Laplace transformation of this equation to find $c(l', p_0)$ is not easy, but a solution compatible with the experimental data can be found by using certain approximations:

$$\frac{1}{p_0 \cosh qL_1} \approx \frac{1}{p_0} - \frac{4}{\pi}\cdot\frac{1}{p_0 + \alpha} + \frac{4}{3\pi}\cdot\frac{1}{p_0 + 9\alpha} \tag{A8}$$

$$\frac{\tanh qL_1}{Dq} \approx \frac{2}{L_1}\cdot\frac{1}{p_0 + \alpha} \tag{A9}$$

These approximations are derived by taking [16] the inverse Laplace transforms of $1/p_0 \cosh qL_1$ and $\tanh qL_1/Dq$ in the form of elliptical theta functions θ_1 and θ_2, respectively, giving a series of exponential functions of time, $\exp(-\alpha t_0)$, $\exp(-9\alpha t_0)$, $\exp(-25\alpha t_0)$, etc., in both instances. Of these, we retain only the first few terms, as the other with the larger exponential coefficients very soon become negligible. Finally, the retained terms are transformed back to give the approximations A8 and A9.

Using these approximations in eqn. A7, and after some rearrangement, this becomes

$$C(l', p_0) = k\left[\frac{p_0 + \alpha}{p_0(p_0 + \alpha + \omega)} - \frac{4}{\pi}\cdot\frac{1}{p_0 + \alpha + \omega} + \frac{4}{3\pi}\cdot\frac{p_0 + \alpha}{(p_0 + 9\alpha)(p_0 + \alpha + \omega)}\right] \tag{A10}$$

where

$$\omega = 2k'_c/L_1 = 2k_c a_L/a_G L_1 \quad \text{(A11)}$$

The inverse transformation of eqn. A10 now gives, after collecting terms of the same exponential function,

$$c(l', t_0) = k\left[\frac{\alpha}{\alpha+\omega} - \left(\frac{4}{\pi} - 1 + \frac{\alpha}{\alpha+\omega} + \frac{4}{3\pi}\cdot\frac{\omega}{8\alpha-\omega}\right)\right.$$
$$\left.\exp[-(\alpha+\omega)t_0] + \frac{4}{3\pi}\cdot\frac{8\alpha}{8\alpha-\omega}\exp(-9\alpha t_0)\right] \quad \text{(A12)}$$

Combining this with eqn. 1 (for $m = 1$), one obtains

$$h = h_\infty - A_1\exp[-(\alpha+\omega)t_0] + A_2\exp(-9\alpha t_0) \quad \text{(A13)}$$

which is the same as eqn. 2.

REFERENCES

1 N. A. Katsanos and G. Karaiskakis, *Adv. Chromatogr.*, 24 (1984) 125.
2 N. A. Katsanos and G. Karaiskakis, *Analyst (London)*, 112 (1987) 809.
3 N. A. Katsanos, *J. Chromatogr.*, 445 (1988) 39.
4 N. A. Katsanos, *Flow Perturbation Gas Chromatography*, Marcel Dekker, New York, Basle, 1988.
5 N. A. Karsanos and J. Kapolos, *Anal. Chem.*, 61 (1989) 2231.
6 N. A. Katsanos, G. Karaiskakis and P. Agathonos, *J. Chromatogr.*, 349 (1986) 369.
7 P. Agathonos and G. Karaiskakis, *Chromatographia*, 25 (1988) 453.
8 P. Agathonos and G. Karaiskakis, *J. Chem. Soc., Faraday Trans. 1*, 85 (1989) 1357.
9 G. Karaiskakis and N. A. Katsanos, *J. Phys. Chem.*, 88 (1984) 3674.
10 M. L. McGlashan and A. G. Williamson, *J. Chem. Soc., Faraday Trans. 1*, 57 (1961) 588.
11 E. Fuller, P. Schettler and J. C. Giddings, *Ind. Eng. Chem.*, 58 (1966) 19.
12 I. M. Elshayal and B. C. Lu, *J. Appl. Chem.*, 18 (1968) 277.
13 J. Gmehling, U. Onken and W. Artl, *Vapor–Liquid Equilibrium Data Collection, Aliphatic Hydrocarbons C7–C18 (Chemistry Data Series*, Vol. 1, Part 6b), University of Dortmund, Dortmund, 1980, p. 246.
14 J. H. Dymond and E. B. Smith, *The Virial Coefficients of Pure Gases and Mixtures —A Critical Compilation*, Clarendon Press, Oxford, 1980.
15 C. Tsonopoulos, *AIChE J.*, 20 (1974) 263.
16 F. Obberhettinger and L. Badii, *Tables of Laplace Transforms*, Springer, Berlin, 1973, pp. 294 and 421.